PROCEEDINGS OF SCIENCE

Investigation of the Ultra-High-Energy gamma-ray emission from the Northern Fermi Bubble with LHAASO-KM2A

Yi Zhang,[a,b,*] **Jiayin He,**[a,b,*] **Rui Zhang**[a,b] **and Shiping Zhao**[a,c]
on behalf of the LHAASO Collaboration
(a complete list of authors can be found at the end of the proceedings)

[a] *Key Laboratory of Dark Matter and Space Astronomy, Purple Mountain Observatory, Chinese Academy of Sciences,*
210023 Nanjing, 9 Jiangsu, China
[b] *University of Science and Technology of China,*
230026 Hefei, Anhui, China
[c] *Institute of Frontier and Interdisciplinary Science, Shandong University,*
266237 Qingdao, Shandong, China

E-mail: zhangyi@pmo.ac.cn, hejy@pmo.ac.cn

We analyze gamma-ray emission from the Northern Fermi bubble region at the ultra-high-energy range, using the data collected by LHAASO-KM2A from December 2019 to September 2022. Employing an improved gamma/hadron separation method, the median energy of the gamma rays is above 25 TeV. We perform the "direct integral method" in the background estimation; however, no significant excess is observed. Consequently, we present the expected upper limits for gamma-ray emissions within the Fermi bubble region at this energy range.

38th International Cosmic Ray Conference (ICRC2023)
26 July - 3 August, 2023
Nagoya, Japan

*Presenter

PoS(ICRC2023)651

1. Introduction

The Fermi bubbles are two large-scale structures of gamma-ray emission situated above and below the Galactic Center, extending to $|b| \sim 50°$. They were initially detected in 2010 using data from the Fermi-LAT telescope[1] and have since been commonly referred to as the "Fermi bubbles". These bubbles exhibit a consistent and uniform spectral index of approximately -2 within the 1 GeV to 100 GeV energy range. The morphology of the Fermi bubbles observed in the gamma-ray band has been identified to be consistent with what has been observed in other wavelengths [2–5]. The formation of the Fermi bubbles and these associated features in different energy bands might have originated from the same past violated event of the Galactic center[1, 5]. Despite discovering the Fermi bubble several years ago, there is ongoing debate regarding their underlying physical mechanisms[6–11]. Notably, observations of the Fermi bubbles in the TeV range have not revealed any significant excess, with upper limits established by HAWC between TeV and 100 TeV[12]. As a portion of the Northern sky region of the Fermi bubble falls within the field of view of LHAASO, our study utilizes the data gathered by LHAASO-KM2A, which has a high sensitivity to ultra-high-energy gamma rays, to investigate gamma-ray emissions from the Northern Fermi bubble region.

2. LHAASO Experiment

The Large High Altitude Air Shower Observatory (LHAASO) is a hybrid ground-based extensive air shower array located at Haizi Mountain in Daocheng, Sichuan province, China ($100.01°E, 29.35°N$, 4410 m a.s.l.) [13]. LHAASO comprises three sub-arrays: a 1.3 square kilometer array (KM2A), a 78000 m^2 water Cherenkov detector array (WCDA), and a wide field of view Cherenkov/fluorescence telescopes array (WFCTA). The construction of the entire KM2A was completed in July 2021, and the full array has been operational since July 20, 2021. The KM2A consists of 5195 electromagnetic detectors (EDs) measuring 1 m^2 each and 1188 muon detectors (MDs) with an area of about 36 m^2 each. KM2A provides unprecedented sensitivity at energies above a few tens of TeV, enabling the search for very- and ultra-high-energy gamma-ray emissions in the northern sky.

3. Data Analysis

In this study, we utilize the data collected during various running periods, specifically from December 27, 2019, to September 30, 2022. These periods include the following: half array (December 27, 2019, to November 30, 2020), three-quarters array (December 1, 2020, to July 19, 2021), and full array (July 20, 2021, to September 30, 2022). The region of interest (ROI) in our study is determined based on the findings of the Fermi bubbles as reported in the paper by [1]. The ROI is restricted to $|b| > 10°$ and covers a declination range of $-20°$ to $4°$, as well as a right ascension range of 220° to 258°. The right panel of Figure 1 provides a visual representation of this region. In addition, it is worth mentioning that the point source of PKS 1510-089 is within the ROI. To exclude any influence from this source, we employ a circular mask with a radius approximately 5 times that of the point spread function (PSF).

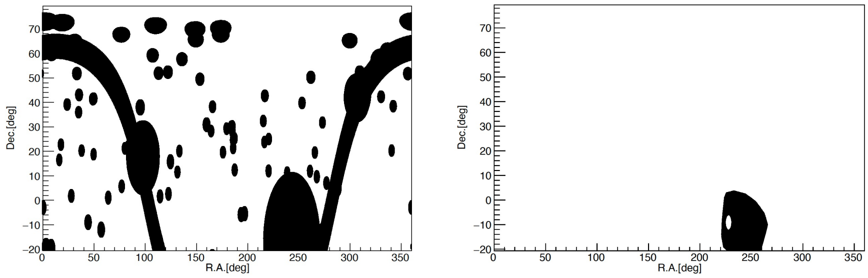

Figure 1: Left) The masked region is in the equatorial coordinate, where the black region is masked in the background estimation procedure. Right) The region of interest (ROI) used in this work, is indicated by the black area.

In the Crab-like point source analysis, we apply the muon selection criteria, ensuring a gamma-ray survival fraction of 90% for energies greater than 100 TeV based on simulations [13]. Given that the Fermi bubble encompasses a substantial solid angle, approximately 0.25 sr, we incorporate additional criteria to effectively reduce the cosmic ray background at higher energies.

The Q factor is defined as the ratio between the survival fraction of gamma rays, ϵ_γ, and the square root of the survival fraction of cosmic ray background, $\epsilon_{\rm CR}$, as shown in

$$Q = \frac{\epsilon_\gamma}{\sqrt{\epsilon_{CR}}}. \tag{1}$$

Both fractions are determined after performing a separation between gamma rays and cosmic rays. The parameter utilized for the separation of gamma rays and hadrons [13] is defined as:

$$R = \log\left(\frac{N_\mu + 0.0001}{N_e}\right) \tag{2}$$

where N_μ represents the number of muons and N_e corresponds to the number of electromagnetic particles in a shower induced by either a gamma ray or a hadron. The comparison of Q obtained from two sets of parameters is shown in Figure 2.

The event selection criteria employed in our study are as follows: Firstly, we require that the triggered EDs and the particles deposited for shower reconstruction exceed a minimum count of ten. Secondly, we impose a condition where the reconstructed direction's zenith angle must be below 50°. Lastly, we restrict the shower age to fall within the range of 0.6 – 2.4. Celestial coordinates bin the data into pixels of size $0.1° \times 0.1°$, while energy bins are logarithmic and equal width $\Delta \log E = 0.4$.

To estimate the background in each pixel, we use the "direct integral method" [14] in this study. This method assumes that the spatial distribution of the collecting efficiency remains stable over a short period in the detector coordinates. We can accurately determine the background by convolving the total event rate with the normalized spatial distribution. We use background data from ±3 hours to estimate the efficiency of the time bin for the central hour.

To reduce the influence of known sources on the background estimation, we exclude the corresponding areas of the sky during the calculation, as shown in Figure 1. We detect sources using LHAASO-KM2A and consider their fitting position, size, and energy distribution, with a

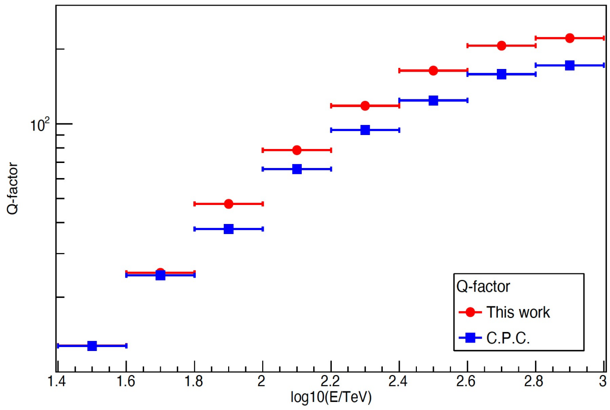

Figure 2: Q-factors at different energy bins for two sets of gamma/hadron separation parameters.

pre-trial significance threshold of 5σ. Each source is assumed to have a two-dimensional Gaussian shape and a power-law spectrum. Furthermore, we also mask the region of interest.

4. Results

By utilizing the "direct integral method," we obtain the counts within the on-source and off-source regions. The significance is determined using the Li-Ma formula. However, no significant excess is detected. Consequently, the upper limits are calculated following the Helene prescription[15]. In our calculations, we assume a power-law spectrum with an index of -2.75 for gamma-ray emissions within the Northern bubble region. Additionally, we assume a uniform flux distribution. The upper limits at the 95% confidence level for each bin are computed, and the results will be presented in the poster. We also employ the equi-zenith angle method for background estimation, yielding consistent results in both significance and upper limits.

In this study, we conduct calculations to determine the expected upper limit for the Fermi Bubble. These calculations were based on the background of KM2A maps, specifically the off-source map. By fluctuating the background events in the off-source maps, we obtained the median value, as well as the 68%, 95%, and 99.7% confidence intervals (CIs). The expected 95% upper limit is represented by the solid-red dashed line in Figure 3, while the color bands represent the 68%, 95%, and 99.7% CIs for the upper limits, denoted as the 1σ, 2σ, and 3σ containment, respectively.

In Figure 3, we present a summary of various observations of the northern Fermi Bubble. Only upper limits on the flux have been provided in the TeV range. It is worth noting that HAWC has recently updated its results based on a template-based search, leading to more stringent constraints compared to its previous findings [16].

The hadronic model, represented by the black line, is based on the work of Lunardini et al. (2015)[18]. This model serves as a gamma-ray counterpart to the neutrino flux model that best fits the data obtained from IceCube. Specifically, IceCube has observed a total of five events that are spatially associated with the Fermi Bubbles. In order to account for the emitted flux from both bubbles, a differential flux model was developed. The resulting upper limits effectively rule out the parent proton spectrum extrapolated from the IceCube data above 100 TeV. The black dashed line

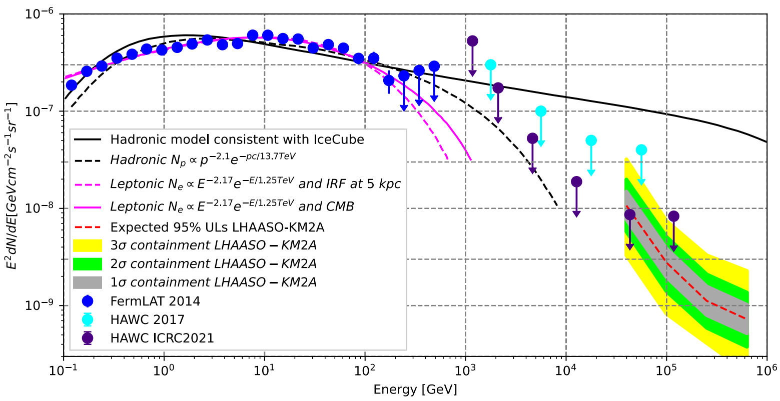

Figure 3: Upper limits on the flux derived from LHAASO-KM2A data, together with data from Fermi, HAWC, and gamma-ray production models proposed by [17] and [18]. The dashed solid-red line represents the predicted limit for the Fermi bubble using KM2A data, while the colored bands depict the 1σ, 2σ, and 3σ containment regions.

represents the hadronic model derived from the research conducted by Ackermann et al. (2014), which assumes a power law with an index of 2.1 and a power law with a cutoff (∼13.7 TeV) for the injection spectrum of the hadrons. These protons interact with the interstellar medium (ISM), producing neutral pions that subsequently decay into gamma rays. On the other hand, the pink lines correspond to the best-fit leptonic models derived from Fermi-LAT data [17], indicating a cutoff energy of approximately 1.25 TeV.

5. Conclusion

The study presents a search for gamma rays with energies above 25 TeV in the region of the Northern Fermi Bubble. A total of 342 days of data from the half array, 232 days from the 3/4 array, and 438 days from the full array of LHAASO-KM2A are utilized in this investigation. No statistically significant excess of gamma rays is observed above 25 TeV within the search area, leading to the calculation of 95% confidence level upper limits on the flux. These upper limits, covering gamma-ray energies ranging from 25 TeV to 1 PeV, contradict the hadronic injection spectrum derived from IceCube measurements. However, the current findings do not provide conclusive evidence regarding the hadronic or leptonic origin of the Fermi bubbles.

6. Acknowledgement

We would like to thank all staff members who work at the LHAASO site above 4400 meters above sea level year-round to maintain the detector and keep the water recycling system, electricity power supply, and other components of the experiment operating smoothly. We are grateful to the Chengdu Management Committee of Tianfu New Area for the constant financial support for research with LHAASO data. This research work is also supported by the following grants: The National Key R&D program of China under grants 2018YFA0404201, 2018YFA0404202, 2018YFA0404203, and 2018YFA0404204, by the National Natural Science Foundation of China No.12273114,No.12022502, No.12205314, No. 12105301, No. 12261160362, No.12105294, No.U1931201, Project for Young Scientists in Basic Research of Chinese Academy of Sciences No. YSBR-061, the Program for Innovative Talents and Entrepreneur in Jiangsu.

References

[1] M. Su, T. R. Slatyer, and D. P. Finkbeiner, The Astrophysical Journal **724**, 1044 (2010).

[2] Y. Sofue, The Astrophysical Journal **540**, 224 (2000).

[3] J. Bland-Hawthorn and M. Cohen, The Astrophysical Journal **582**, 246 (2003).

[4] D. P. Finkbeiner, The Astrophysical Journal **614**, 186 (2004).

[5] J. Bland-Hawthorn, P. R. Maloney, R. Sutherland, B. Groves, M. Guglielmo, W. Li, A. Curzons, G. Cecil, and A. J. Fox, The Astrophysical Journal **886**, 45 (2019).

[6] R. M. Crocker and F. Aharonian, Phys. Rev. Lett. **106**, 101102 (2011).

[7] K. Zubovas, A. R. King, and S. Nayakshin, Monthly Notices of the Royal Astronomical Society: Letters **415**, L21 (2011).

[8] H.-Y. K. Yang, M. Ruszkowski, and E. Zweibel, Monthly Notices of the Royal Astronomical Society **436**, 2734 (2013).

[9] K. C. Sarkar, B. B. Nath, and P. Sharma, Monthly Notices of the Royal Astronomical Society **467**, 3544 (2017).

[10] G. Mou, D. Sun, T. Fang, W. Wang, R. Zhang, F. Yuan, Y. Sofue, T. Wang, and Z. He, Nature Communications **14**, 781 (2023).

[11] R. Zhang and F. Guo, The Astrophysical Journal **894**, 117 (2020).

[12] A. U. Abeysekara, A. Albert, R. Alfaro, C. Alvarez, J. D. Álvarez, R. Arceo, J. C. Arteaga-Velázquez, H. A. A. Solares, A. S. Barber, N. Bautista-Elivar, et al., The Astrophysical Journal **842**, 85 (2017).

[13] F. Aharonian, Q. An, Axikegu, L. X. Bai, Y. X. Bai, Y. W. Bao, D. Bastieri, X. J. Bi, Y. J. Bi, H. Cai, et al., Chinese Physics C **45**, 025002 (2021).

[14] R. Atkins, W. Benbow, D. Berley, E. Blaufuss, J. Bussons, D. G. Coyne, R. S. Delay, T. DeYoung, B. L. Dingus, D. E. Dorfan, et al., The Astrophysical Journal **595**, 803 (2003).

[15] O. Helene, Nuclear Instruments and Methods in Physics Research **212**, 319 (1983).

[16] P. Surajbali, *A Novel Approach towards the Search for Gamma-ray Emission from the Northern Fermi Bubble with HAWC* (2021), arXiv:2107.14553 [astro-ph].

[17] M. Ackermann, A. Albert, W. B. Atwood, L. Baldini, J. Ballet, G. Barbiellini, D. Bastieri, R. Bellazzini, E. Bissaldi, R. D. Blandford, et al., The Astrophysical Journal **793**, 64 (2014).

[18] C. Lunardini, S. Razzaque, and L. Yang, Phys. Rev. D **92**, 021301 (2015).

Full Authors List: LHAASO Collaboration

Zhen Cao[1,2,3], F. Aharonian[4,5], Q. An[6,7], Axikegu[8], Y.X. Bai[1,3], Y.W. Bao[9], D. Bastieri[10], X.J. Bi[1,2,3], Y.J. Bi[1,3], J.T. Cai[10], Q. Cao[11], W.Y. Cao[7], Zhe Cao[6,7], J. Chang[12], J.F. Chang[1,3,6], A.M. Chen[13], E.S. Chen[1,2,3], Liang Chen[14], Lin Chen[8], Long Chen[8], M.J. Chen[1,3], M.L. Chen[1,3,6], Q.H. Chen[8], S.H. Chen[1,2,3], S.Z. Chen[1,3], T.L. Chen[15], Y. Chen[9], N. Cheng[1,3], Y.D. Cheng[1,3], M.Y. Cui[12], S.W. Cui[11], X.H. Cui[16], Y.D. Cui[17], B.Z. Dai[18], H.L. Dai[1,3,6], Z.G. Dai[7], Danzengluobu[15], D. della Volpe[19], X.Q. Dong[1,2,3], K.K. Duan[12], J.H. Fan[10], Y.Z. Fan[12], J. Fang[18], K. Fang[1,3], C.F. Feng[20], L. Feng[12], S.H. Feng[1,3], X.T. Feng[20], Y.L. Feng[15], S. Gabici[21], B. Gao[1,3], C.D. Gao[20], L.Q. Gao[1,2,3], Q. Gao[15], W. Gao[1,3], W.K. Gao[1,2,3], M.M. Ge[18], L.S. Geng[1,3], G. Giacinti[13], G.H. Gong[22], Q.B. Gou[1,3], M.H. Gu[1,3,6], F.L. Guo[14], X.L. Guo[8], Y.Q. Guo[1,3], Y.Y. Guo[12], Y.A. Han[23], H.H. He[1,2,3], H.N. He[12], J.Y. He[12], X.B. He[17], Y. He[8], M. Heller[19], Y.K. Hor[17], B.W. Hou[1,2,3], C. Hou[1,3], X. Hou[24], H.B. Hu[1,2,3], Q. Hu[7,12], S.C. Hu[1,2,3], D.H. Huang[8], T.Q. Huang[1,3], W.J. Huang[17], X.T. Huang[20], X.Y. Huang[12], Y. Huang[1,2,3], Z.C. Huang[8], X.L. Ji[1,3,6], H.Y. Jia[8], K. Jia[20], K. Jiang[6,7], X.W. Jiang[1,3], Z.J. Jiang[18], M. Jin[8], M.M. Kang[25], T. Ke[1,3], D. Kuleshov[26], K. Kurinov[26,27], B.B. Li[11], Cheng Li[6,7], Cong Li[1,3], D. Li[1,2,3], F. Li[1,3,6], H.B. Li[1,3], H.C. Li[1,3], H.Y. Li[7,12], J. Li[7,12], Jian Li[7], Jie Li[1,3,6], K. Li[1,3], W.L. Li[20], W.L. Li[13], X.R. Li[1,3], Xin Li[6,7], Y.Z. Li[1,2,3], Zhe Li[1,3], Zhuo Li[28], E.W. Liang[29], Y.F. Liang[29], S.J. Lin[17], B. Liu[7], C. Liu[1,3], D. Liu[20], H. Liu[8], H.D. Liu[23], J. Liu[1,3], J.L. Liu[1,3], J.Y. Liu[1,3], M.Y. Liu[15], R.Y. Liu[9], S.M. Liu[8], W. Liu[1,3], Y. Liu[10], Y.N. Liu[22], R. Lu[18], Q. Luo[17], H.K. Lv[1,3], B.Q. Ma[28], L.L. Ma[1,3], X.H. Ma[1,3], J.R. Mao[24], Z. Min[1,3], W. Mitthumsiri[30], H.J. Mu[23], Y.C. Nan[1,3], A. Neronov[21], Z.W. Ou[17], B.Y. Pang[8], P. Pattarakijwanich[30], Z.Y. Pei[10], M.Y. Qi[1,3], Y.Q. Qi[11], B.Q. Qiao[1,3], J.J. Qin[7], D. Ruffolo[30], A. Sáiz[30], D. Semikoz[21], C.Y. Shao[17], L. Shao[11], O. Shchegolev[26,27], X.D. Sheng[1,3], F.W. Shu[31], H.C. Song[28], Yu.V. Stenkin[26,27], V. Stepanov[26], Y. Su[12], Q.N. Sun[8], X.N. Sun[29], Z.B. Sun[32], P.H.T. Tam[17], Q.W. Tang[31], Z.B. Tang[6,7], W.W. Tian[2,16], C. Wang[32], C.B. Wang[8], G.W. Wang[7], H.G. Wang[10], H.H. Wang[17], J.C. Wang[24], K. Wang[9], L.P. Wang[20], L.Y. Wang[1,3], P.H. Wang[8], R. Wang[20], W. Wang[17], X.G. Wang[29], X.Y. Wang[9], Y. Wang[8], Y.D. Wang[1,3], Y.J. Wang[1,3], Z.H. Wang[25], Z.X. Wang[18], Zhen Wang[13], Zheng Wang[1,3,6], D.M. Wei[12], J.J. Wei[12], Y.J. Wei[1,2,3], T. Wen[18], C.Y. Wu[1,3], H.R. Wu[1,3], S. Wu[1,3], X.F. Wu[12], Y.S. Wu[7], S.Q. Xi[1,3], J. Xia[7,12], J.J. Xia[8], G.M. Xiang[2,14], D.X. Xiao[11], G. Xiao[1,3], G.G. Xin[1,3], Y.L. Xin[8], Y. Xing[14], Z. Xiong[1,2,3], D.L. Xu[13], R.F. Xu[1,2,3], R.X. Xu[28], W.L. Xu[25], L. Xue[20], D.H. Yan[18], J.Z. Yan[12], T. Yan[1,3], C.W. Yang[25], F. Yang[11], F.F. Yang[1,3,6], H.W. Yang[17], J.Y. Yang[17], L.L. Yang[17], M.J. Yang[1,3], R.Z. Yang[7], S.B. Yang[18], Y.H. Yao[25], Z.G. Yao[1,3], Y.M. Ye[22], L.Q. Yin[1,3], N. Yin[20], X.H. You[1,3], Z.Y. You[1,2,3], Y.H. Yu[7], Q. Yuan[12], H. Yue[1,2,3], H.D. Zeng[12], T.X. Zeng[1,3,6], W. Zeng[18], M. Zha[1,3], B.B. Zhang[9], F. Zhang[8], H.M. Zhang[9], H.Y. Zhang[1,3], J.L. Zhang[16], L.X. Zhang[10], Li Zhang[18], P.F. Zhang[18], P.P. Zhang[7,12], R. Zhang[7,12], S.B. Zhang[2,16], S.R. Zhang[11], S.S. Zhang[1,3], X. Zhang[9], X.P. Zhang[1,3], Y.F. Zhang[8], Yi Zhang[1,12], Yong Zhang[1,3], B. Zhao[8], J. Zhao[1,3], L. Zhao[6,7], L.Z. Zhao[11], S.P. Zhao[12,20], F. Zheng[32], B. Zhou[1,3], H. Zhou[13], J.N. Zhou[14], M. Zhou[31], P. Zhou[9], R. Zhou[25], X.X. Zhou[8], C.G. Zhu[20], F.R. Zhu[8], H. Zhu[16], K.J. Zhu[1,2,3,6], X. Zuo[1,3], (The LHAASO Collaboration)

[1] Key Laboratory of Particle Astrophysics & Experimental Physics Division & Computing Center, Institute of High Energy Physics, Chinese Academy of Sciences, 100049 Beijing, China
[2] University of Chinese Academy of Sciences, 100049 Beijing, China
[3] TIANFU Cosmic Ray Research Center, Chengdu, Sichuan, China
[4] Dublin Institute for Advanced Studies, 31 Fitzwilliam Place, 2 Dublin, Ireland
[5] Max-Planck-Institut for Nuclear Physics, P.O. Box 103980, 69029 Heidelberg, Germany
[6] State Key Laboratory of Particle Detection and Electronics, China
[7] University of Science and Technology of China, 230026 Hefei, Anhui, China
[8] School of Physical Science and Technology & School of Information Science and Technology, Southwest Jiaotong University, 610031 Chengdu, Sichuan, China
[9] School of Astronomy and Space Science, Nanjing University, 210023 Nanjing, Jiangsu, China
[10] Center for Astrophysics, Guangzhou University, 510006 Guangzhou, Guangdong, China
[11] Hebei Normal University, 050024 Shijiazhuang, Hebei, China
[12] Key Laboratory of Dark Matter and Space Astronomy & Key Laboratory of Radio Astronomy, Purple Mountain Observatory, Chinese Academy of Sciences, 210023 Nanjing, Jiangsu, China
[13] Tsung-Dao Lee Institute & School of Physics and Astronomy, Shanghai Jiao Tong University, 200240 Shanghai, China
[14] Key Laboratory for Research in Galaxies and Cosmology, Shanghai Astronomical Observatory, Chinese Academy of Sciences, 200030 Shanghai, China
[15] Key Laboratory of Cosmic Rays (Tibet University), Ministry of Education, 850000 Lhasa, Tibet, China
[16] National Astronomical Observatories, Chinese Academy of Sciences, 100101 Beijing, China
[17] School of Physics and Astronomy (Zhuhai) & School of Physics (Guangzhou) & Sino-French Institute of Nuclear Engineering and Technology (Zhuhai), Sun Yat-sen University, 519000 Zhuhai & 510275 Guangzhou, Guangdong, China
[18] School of Physics and Astronomy, Yunnan University, 650091 Kunming, Yunnan, China
[19] Département de Physique Nucléaire et Corpusculaire, Faculté de Sciences, Université de Genève, 24 Quai Ernest Ansermet, 1211 Geneva, Switzerland
[20] Institute of Frontier and Interdisciplinary Science, Shandong University, 266237 Qingdao, Shandong, China
[21] APC, Universit'e Paris Cit'e, CNRS/IN2P3, CEA/IRFU, Observatoire de Paris, 119 75205 Paris, France
[22] Department of Engineering Physics, Tsinghua University, 100084 Beijing, China
[23] School of Physics and Microelectronics, Zhengzhou University, 450001 Zhengzhou, Henan, China
[24] Yunnan Observatories, Chinese Academy of Sciences, 650216 Kunming, Yunnan, China

[25] College of Physics, Sichuan University, 610065 Chengdu, Sichuan, China
[26] Institute for Nuclear Research of Russian Academy of Sciences, 117312 Moscow, Russia
[27] Moscow Institute of Physics and Technology, 141700 Moscow, Russia
[28] School of Physics, Peking University, 100871 Beijing, China
[29] School of Physical Science and Technology, Guangxi University, 530004 Nanning, Guangxi, China
[30] Department of Physics, Faculty of Science, Mahidol University, 10400 Bangkok, Thailand
[31] Center for Relativistic Astrophysics and High Energy Physics, School of Physics and Materials Science & Institute of Space Science and Technology, Nanchang University, 330031 Nanchang, Jiangxi, China
[32] National Space Science Center, Chinese Academy of Sciences, 100190 Beijing, China